Research Journal of Applied Sciences, Engineering and Technology 4(15): 2323-2333, 2012
ISSN: 2040-7467

Submitted: December 23, 2011 Accepted: January 21, 2012 Published: August 01, 2012

# Parametric Design and Robust Control Strategy for HEV Based on Permanent Magnet Electrical Variable Transmission

Abdelsalam Ahmed and Shumei Cui
Department of Electrical Machines and Automation, Harbin Institute of Technology, China

**Abstract:** In this study, Permanent Magnet-Dual Mechanical Ports (PM-DMP) machine is used as an Electrical Variable Transmission (EVT), instead the Toyota Hybrid System (THS) transmission, in Hybrid Electric Vehicle (HEV). Decreasing and exploiting the power ratings of the power plants in the HEV system are the most efficient factors for increasing the economy and efficiency of the system. These goals are achieved through three tandem procedures: the first is focusing on the detailed calculations of the power ratings for the PMSM-EVT machines. These calculations are mainly based on the deeply analysis of the function of each plant at steady and dynamic states. The second is the robust vector control of the two PMSMs with the field weakening strategy. The third is developing a robust global power management control strategy to realize the power splitting for the full hybrids. The integration of HEV components including their dynamic models and controllers has been implemented by Energetic Macroscopic Representation (EMR) simulation tool. The goals are validated by the simulation results with two different driving cycles; and from the interim analytical calculations and from analyzing the simulation results, the rated and maximum specifications of the PMSM-EVT have been defined. Finally, the results are validated by comparing to the practical data of the Toyota Prius HEV. The results show that the power ratings of the electrical machines are saved more than that of Prius machines. Also, the system is driven at harder burden loads than that of Prius with perfect drivability.

**Keywords:** Electrical variable transmission, energetic macroscopic representation, global power management control strategy, hybrid electric vehicle, permanent magnet-dual mechanical ports

## INTRODUCTION

Toyota Hybrid System (THS) transmission in Toyota Prius Hybrid Electric Vehicle (HEV) acts as an energy split unit in which a traction drive motor, electrical generator and planetary gear set are organized (ADVISOR, 2002; Liu *et al*., 2005). However, this planetary-geared as an Electrical Variable Transmission (EVT) system inherits the fundamental drawbacks of planetary gearing, namely, transmission loss, gear noise and need of regular lubrication (Chau *et al*., 2008).

In recently, many active research studies are still interesting to replace this THS while retaining the EVT propulsion (Kruse *et al*., 2006; Chen *et al*., 2009; Cheng *et al*., 2011). The permanent magnet EVT as a compact, multifunctional device with its functionality of a continuously variable transmission replaced the standard automatic transmission (Kruse *et al*., 2006). Also, a Dual Mechanical Port (DMP) machine as an energy conversion device has been introduced as an alternative to Toyota's THS transmission in Chen *et al*. (2009).

Across many years, many research studies have been done about the power parameters' matching design for HEV components based on the EVT. The specifications of the PMSM-DMP were defined in Fan *et al*. (2008). In Guo *et al*. (2008), the power parameters matching design of the DMPM was presented considering the equality of rated and the maximum powers and torques for the inner machine of EVT. Also, the rated power parameters' matching design of DMPM was discussed in Zhuang *et al*. (2009) considering the economic zone of the ICE and the power compensation effect of battery. In Cheng *et al*. (2008), the rated power parameters for EVT motors are decided from the information of the working points' distribution and the area where there are the densest working points of motor is considered as the rated working points. In addition, the technical requirements for the design of PMSM-EVT was defined and analyzed in Cheng *et al*. (2011) replacing the THS transmission with the PM-EVT.

Many types of electrical machines have been researched as an EVT, for induction machines (Cheng *et al*., 2008; Chen *et al*., 2008a). Recently, the permanent magnet machines are chosen as EVT in HEVs because of its higher efficiency and torque density (Chau *et al*., 2008; Cheng *et al*., 2011).

Energetic Macroscopic Representation (EMR), as a graphical modeling and simulation tool, has been introduced to describe HEV in Chen *et al*. (2008b), Cheng *et al*. (2008) and Chen *et al*. (2008a) used EMR and its inversion method for modeling and control HEV based on induction machines-EVT.

**Corresponding Author:** Abdelsalam Ahmed, Department of Electrical Machines and Automation, Harbin Institute of Technology, China

The rule-based revised control strategy has been used to coordinate the power distribution process between the components of HEV (Cheng *et al*., 2008; Chen *et al*., 2008a).

This study focuses on three main aspects: the first is the power rating designs of subsystems composing to the studied PMSM-EVT-HEV. The most operating conditions, covering the steady and dynamic states of the PMSM-EVT machines, are considered. Second, Using the EMR methodology, the integrating of the components of the studied HEV and deducing their local controllers are accomplished. The field oriented control of the PM-EVT machines is developed. This local vector control considers the strategy of field weakening control to extend the operation of the electrical machines and hence the vehicle at the constant power areas. Finally, the rule-based power follower control strategy applied to that HEV presented previously in Cheng *et al*. (2008). Cheng *et al*. (2008) is modified and improved according to the power rating designs of the components; and also PM machines are used in state of induction machines. This strategy guarantees the optimum operation for the ICE, sustaining SOC of the battery, distribute the requested power at the wheels between the power plants and finally save the power ratings of the PM machines.

## PMSM-EVT-HEV SYSTEM

**System structure:** Permanent magnet DMP is used as an EVT unit in the studied HEV, as shown in Fig. 1. That PMSM-EVT system consists of two permanent magnet synchronous machines EM1 and EM2.

The stator of EM1 is connected to the ICE shaft to rotate at the same speed $\Omega_{m1}$ and the rotor is coupled with the rotor of the EM2 to rotate at the same speed $\Omega_{m2}$. The two rotors have permanent magnet and the two stators have three phase windings connected to power supply via two inverters. The electromagnetic torque of EM1 is developed according to the speed difference between the inner and outer rotors, whereas the EM2 is considered mature PMSM.

EVT unit is used as a Continuously Variable Transmission (CVT), motor and generator to replace the Toyota Hybrid System (THS) in the Toyota Prius HEV. So with the aid of the field weakening vector control, the PM-EVT machines are exploited to optimize the ICE operation via covering the speed and torque difference between the vehicle requirements and the optimized output of the engine. The EVT, ICE, battery and final gear are the main components of the studied HEV.

In this study, the ICE, battery, power inverters, vehicle dynamics and transmission have been modeled and simulated according to the typical data of the well-known Toyota prius HEV obtained from the (ADVISOR, 2002), as listed in Table 1. These plants have been

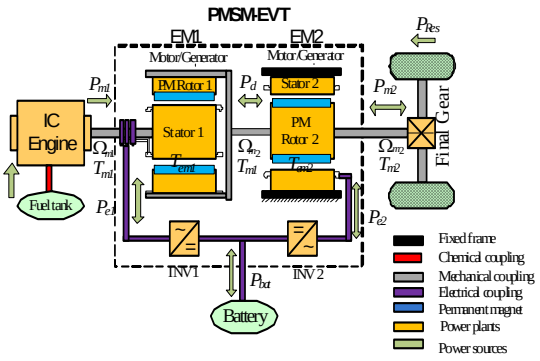


Fig. 1: Hybrid electric vehicle driven with PMSM-EVT

Table 1: Vehicle and environmental parameters

| Component variables | Symbol | Value | Unit |
|---|---|---|---|
| Final drive gear, | $K_{gear}$ | 3.93 | |
| Gravity, | $g$ | 9.81 | m/s^2 |
| Air density | $\rho$ | 1.2 | kg/m^3 |
| Total mass | $M_{veh}$ | 1368 | kg |
| Vehicle velocity | $V_{veh}$ | 70.75 | km/h |
| Max. acceleration | | 1.19 | m/s2 |
| Aerodynamic drag coefficient | $C_d$ | 0.3 | |
| Frontal area of vehicle | $S_f$ | 1.746 | m^2 |
| Rolling radius of tire | $R_w$ | 0.287 | m |
| Rolling resistance coefficient | $V_f$ | 0.0165 | |

modeled and simulated via EMR, more details could be found in Chen *et al*. (2008a). Also the regenerative braking force is considered as a constant ratio from the total braking force according to the power ratings of the EVT machines. In this study, the regenerative power part has been taken as 60% from the total braking power to test the maximum limits of the PM machines.

**Power required from the drive train system:** The ratings design of EVT machines are done at the worst road conditions to test the maximum boundaries. So, in this method the maximum road requirements from the traction drive machine is to run at maximum velocity of 70 Km/h at the maximum acceleration of 1.19 m/s$^2$. The maximum vehicle power required from the power train (ICE and EVT machines) at the wheels can be calculated as:

$$P_m = \frac{V_{veh}}{\eta_T}\left(M_{veh} g \sin\alpha + \frac{1}{2}\rho C_d S_f \upsilon_{veh}^2 + M_{veh} g V_f \cos\alpha + 1.15 M_{veh}\frac{d\upsilon_{veh}}{dt}\right) \quad (1)$$

Substituting in (1) and with the aid of the parameters of HEV listed in the Table 1, the maximum required power of the vehicle is43.03kW.

The total driving load torque required from the drivetrain (both ICE and EVT machines), is calculated using (2).

$$T_m = \frac{1000 R_w}{K_g V_{veh}} P_m \quad (2)$$

Substituting in (2), the maximum required torque of the vehicle is 160 Nm.

## PARAMETRIC DESIGN OF THE PMSM-EVT MACHINES

Parameters of the series/parallel (speed/torque couplings) hybrid drive train such as engine power, electric machines power, gear ratio of transmission and power and energy capacity of the energy storage system are key parameters and exert considerable influence on vehicle performance and operation efficiency. However, as initial steps in the drive train design, these parameters should be estimated based on vehicle performance requirements.

Such parameters should also be refined by more accurate simulations. In this study, the parameters of a Toyota Prius passenger car are used in calculations. Because of all plants of the system make together via the power management strategy, so as an essential base, this strategy has to be considered on power matching determination of power plants. Also, studying the predicted regenerative energy from the vehicle, which is related to the vehicle, driver and road conditions, represents main factor on designing procedure.

**Maximum and rated speeds of EM2:** The maximum velocity of Prius HEV of 70.75 Km/h is taken as the maximum continuous speed of EM2. Almost, this speed is designed to be lesser than the maximum speed and bigger than the rated value. By reviewed to the CYC 1015 Prius and with the aid of (3), the rated speed can be taken as $\Omega_{m2}$ = 180 rad/sec (1720 rpm) that related to 50 km/h to represent the final urban velocity and initial highway stage:

$$N_m = \frac{30}{\pi} \frac{K_{gear}}{R_w} \upsilon_{veh} \quad (3)$$

And because of the PM machines have a small speed ratio, defined as the ratio of its maximum speed to the base speed, because of difficulty of field weakening due to the performance of the permanent magnet (Ehsani *et al*., 2010), the maximum speed of EM2 is taken as $\Omega_{em2\text{-}max} = 2.5\Omega_{m2\_rated}$ = 450 rad/sec = 4300 rpm.

**Maximum and rated speeds of EM1:** The EM1 is controlled via vector control to compensate the speed requirements of vehicle that deviated to the ICE optimal speeds. Therefore, choosing the power ratings of EM1 depends on the speed difference between the inner and the outer rotors. The effective speed and the developed power for EM1 are calculated.

Table 2: Speed ratings of EM1 at vehicle velocity of 70.75 km/h

| ICE:$N_{m1}$ (rpm) | EM2:$N_{m2}$ (rpm) | EM1:$N_{em1}$ (rpm) | Operation states |
|---|---|---|---|
| Max = 3972 | Max = 2578 | 1394 | EM1 generator, EM2 motor |
| | Min = 0 | 3972 | Vehicle stopping, EM1 generator, EM2 motor |
| Min = 1200 | Max = 2578 | 1378 | EM1 generator, EM2 motor |
| | Min = 0 | 1200 | Barking with charging battery |
| 0 | Max = 2578 | 2578 | $V_{veh}$ very high, EM1 motor, EM2 motor, |
| | Min = 0 | 0 | Barking, rest |

$$\Omega_{em1} = \Omega_{m1} - \Omega_{m2} \quad (4)$$

Substituting in Eq. (4) with minimum and maximum values of EM1 and EM2 speeds, Table 2 lists the all possible operational modes showing numerically all different cases of the effective speed of EM1 by which the rated and maximum speeds would be determined.

From Table 2, it can be noted that, the maximum logical slip speed between the engine and the vehicle defines the maximum speed of EM1. Because of case 2 represents the worst operating instant on any driving cycle and it is considered as an illogical operating case, the vehicle control strategy has to prevent this situation to happen, therefore it has not been taken as maximum value. And hence, the speed of 188 rad/sec or 2578 rpm has been taken as the maximum speed of the EM1. Due to frequently stop-go, variation of driving cycle all time and different operating conditions of ICE and battery operation, the speed of 144.3 rad/sec or 1378 rpm could be considered as the wide operation speed. And hence, it is used as rated value of EM1.

**Maximum and rated torques of EM1:** Considering the engine torque and dynamic characteristics of the inner shaft, the maximum developed torque required from EM1 has to be greater than that of the maximum engine torque and could be estimated as (5):

$$T_{em1-\max} = T_{ICE-\max} + J\left(\frac{d\Omega_{ICE}}{dt}\right)_{\max} \quad (5)$$

The maximum torque can be delivered by the ICE is $T_{ICE\text{-}max}$ = 103 Nm and taking the inertia of the ICE and inner rotor into consideration, the maximum torque of EM1 is 105 Nm. By using the minimum optimum torque of the engine (55 Nm), the rated torque for EM1 is determined as 60 Nm:

$$P_{em1} = T_{em1}\, \Omega_{em1} \quad (6)$$

According to Eq. (6), the rated and maximum powers then could be calculated:

$$P_{em1-rated} \cong 8.66kW \text{ and } P_{em1-\max} \cong 15.15kW$$

**Maximum and rated torques of EM2:** Referring to the previous subsections, the maximum vehicle torque at the

Table 3: Specifications of EM1 and EM2 from the calculations: torque (Nm), speed (rpm), power (kW)

| | Optimum ICE | | | EM1 | | | Transmitted | | | EM2 | | | Output | | |
|---|---|---|---|---|---|---|---|---|---|---|---|---|---|---|---|
| | $T_{m1}$ | $N_{m1}$ | $P_{m1}$ | $T_{em1}$ | $N_{em1}$ | $P_{em1}$ | $T_t$ | $N_t$ | $P_t$ | $T_{em2}$ | $N_{em2}$ | $P_{em2}$ | $T_{m2}$ | $N_{m2}$ | $P_{m2}$ |
| Min. | 55 | 1200 | 7 | 60 | 1378 | 8.66 | 60 | 1720 | 10.8 | 80 | 1720 | 14.4 | 0 | 0 | 0 |
| Max. | 96 | 3972 | 40 | 105 | 2578 | 15.15 | 105 | 4300 | 18.9 | 160 | 4300 | 28.8 | 160 | 2578 | 43.19 |

motor side, at the worst conditions, $T_{m2\text{-}max}$ is calculated as 160 Nm. From the torque calculations of EM1 and the torque at the wheels, maximum torque of EM2 is mainly defined from (7):

$$T_{em2\_max} = T_{m2\_max} - T_{em1\_min} \quad (7)$$

Substituting in (7), the first calculated maximum torque for the EM2 is 160-60 = 100 Nm. But practically the maximum torque of EM2 is affected strongly by many effective factors:

- Considering the dynamic process of vehicle motion the maximum torque of EM2 has to be increased.
- At the same time, very important issue of regenerative (negative) torque has to be taken into account because of at many times the deceleration power exceeds the traction power. And with the decreasing of the velocity of vehicle, the braking torque increases rapidly; and hence, the maximum torque of EM2 has to be increased.
- Also, the operating torque of ICE affects strongly on the torque of EM2. When the ICE operates at its maximum torque while the vehicle runs slowly, maximum negative torque applied to EM2. And as soon as the vehicle moves more, this torque decreases.
- Practically, it is expected to start the vehicle with its maximum gradeability or maximum acceleration while the ICE turns OFF. At those instants, maximum torque has to be developed by just EM2 is 160 Nm.

Considering the all mentioned operating factors, $T_{em2\text{-}max}$ = 160 Nm is the saved torque to the drivability of the system; and $T_{em2\_rated} = 0.5\ T_{em2\_max}$ = 80Nm. The maximum and rated operating powers of EM2 are25.2 KW and13 KW.

**Transmitted power from the EM1 to the EM2:** Transmitted power from the EM1 to the EM2 can be calculated using the following relations:

$$T_t = T_{em1}$$
$$N_t = N_{em2}$$
$$P_t = T_{em1}\omega_{em2} \quad (8)$$

All the calculated data, that deduced from understanding the system structure and operational functions for each power plant in the system, are listed in Table 3.

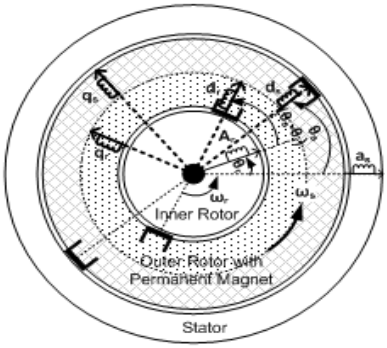


Fig. 2: Reference frame for the SM and DR PM machines

## EMR MODEL AND CONTROL OF PMSM-EVT-HEV SYSTEM

**EMR model of the PMSM:** With neglecting the magnetic field interference in the air gap between EM1 and EM2, the used PM-EVT is considered as two PMSMs. One is the conventional machine, EM2 and the other is double rotor machine (DRM), EM1. The reference frame for the two machines is studied in a general d-q rotating reference frame as shown in Fig. 2. The DRM in Fig. 2 is represented by the inner rotor and the inner side of the outer rotor with permanent magnet that rotates with $\omega_r$.The three phases windings of EM1 machine is referred to the rotating reference frame $dq_r$ with the electrical angle of $\Delta\theta = \theta_s - \theta_r$ ;whereas the three phases windings of EM2 machine is referred to the rotating reference frame $dq_s$ with the angle of $\theta_s$ .

The EMR model of the DR-PMSM machine has been depicted in three stages.

**Park transformation t($\Delta\ \theta$):** That expresses stator voltages $u_s$ and stator currents $i_s$ in the (d, q) rotating reference frame:

$$v_{sdq} = [T(\Delta\ \theta_s)]u_s \quad (9)$$

$$i_s = \left[T(\Delta\theta_s)\right]^{-1} i_{sdq} \quad (10)$$

where, $\theta_s$ is the rotor position with respect to the stator frame.

**Stator windings:** Impose the stator current $i_{sdq}$as state variables from the stator voltages $v_{sdq}$ and E.M.F.$e_{sdq}$.

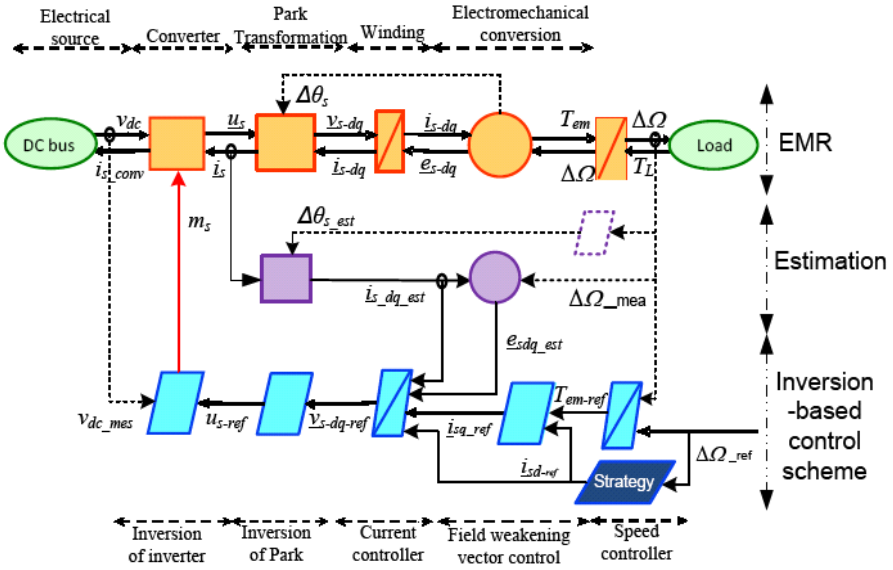


Fig. 3: EMR and its inversion-based control of PMSM

$$\upsilon_{sdq} - e_{sdq} - \left(i_{sdq} * R_s\right) = L_{dq}\frac{d}{dt}\left(i_{sdq}\right) \quad (11)$$

where, $R_s$, $L_d$ and $L_q$ are the stator resistance and d-q inductances of PMSM, respectively.

**The electromechanical conversion:** leads to the machine torque $T_{em}$ and the B.EMF $e_{sdq}$ from the stator currents and the rotation speed as (12) to (16):

$$T_{em} = 3/2pi_q[\varphi_e + (L_d - L_q)i_d] \quad (12)$$

$$e_{sd} = -\varphi_d(\omega_r - \omega_s) \quad (13)$$

$$e_{sq} = \varphi_q(\omega_r - \omega_s) \quad (14)$$

$$\varphi_d = L_q\, i_q \quad (15)$$

$$\varphi_q = L_d\, i_d + \varphi_e \quad (16)$$

where, $\varphi_d$, $\varphi_q$, $i_d$ and $i_q$ the flux linkage and current components in d-q directions, $\omega_r$ and $\omega_s$ denote the electrical angular speeds for inner rotor and outer rotor, respectively, $p$ number of pole pairs and $\varphi_e$ flux linkage of the permanent magnet. The EMR simulation model is shown in the upper part of Fig. 3. The EMR modeling for the EM2 is the same as that of the DR machine with a fixed stator.

**Maximum control structure vector control of DR-PMSM with field weakening control:** The MCS considers all the theoretical calculations and measurements required by direct inversion of the obtained EMR. To deduce the MCS, the different control objectives have to be first identified. Then the EMR blocks are inverted regardless of practical issues: the conversion blocks are directly inverted and the accumulation blocks are inverted using controllers in order to respect physical causality.

Due to the big necessary of extending the speed rage, field oriented control with the possibility of field weakening has been used for both EM1 and EM2. This procedure basically deals with the magnetic and torque component current as shown in the lower part of Fig. 3.

**The reference current $i_{q\_ref}$:** the inversion of torque Eq. (12) leads to the reference current $i_{sq\text{-}ref}$ from the torque reference $T_{em\_ref}$:

$$i_{sq\_ref} = \frac{T_{em\_ref}}{\frac{3}{2}p\left[\varphi_e + \left(L_d - L_q\right)i_{d\_ref}\right]} \quad (17)$$

**The reference current $i_{d\_ref}$ :** Also, the reference current $i_{sd\_ref}$ is forced to zero under the base speed and then forced to negative value related to the speed as soon as it exceeds the base speed (Krishnan, 2010):

$$i_{sd-ref} = \begin{cases} \dfrac{\varphi_e}{L_d}\left(\dfrac{(\omega_r - \omega_s)_{base}}{(\omega_r - \omega_s)} - 1\right) & \omega_r \geq \omega_{base} \\ 0 & \omega_r \leq \omega_{base} \end{cases} \quad (18)$$

**Current controllers:** are required to invert current relationships that deduced from windings Eq. (19):

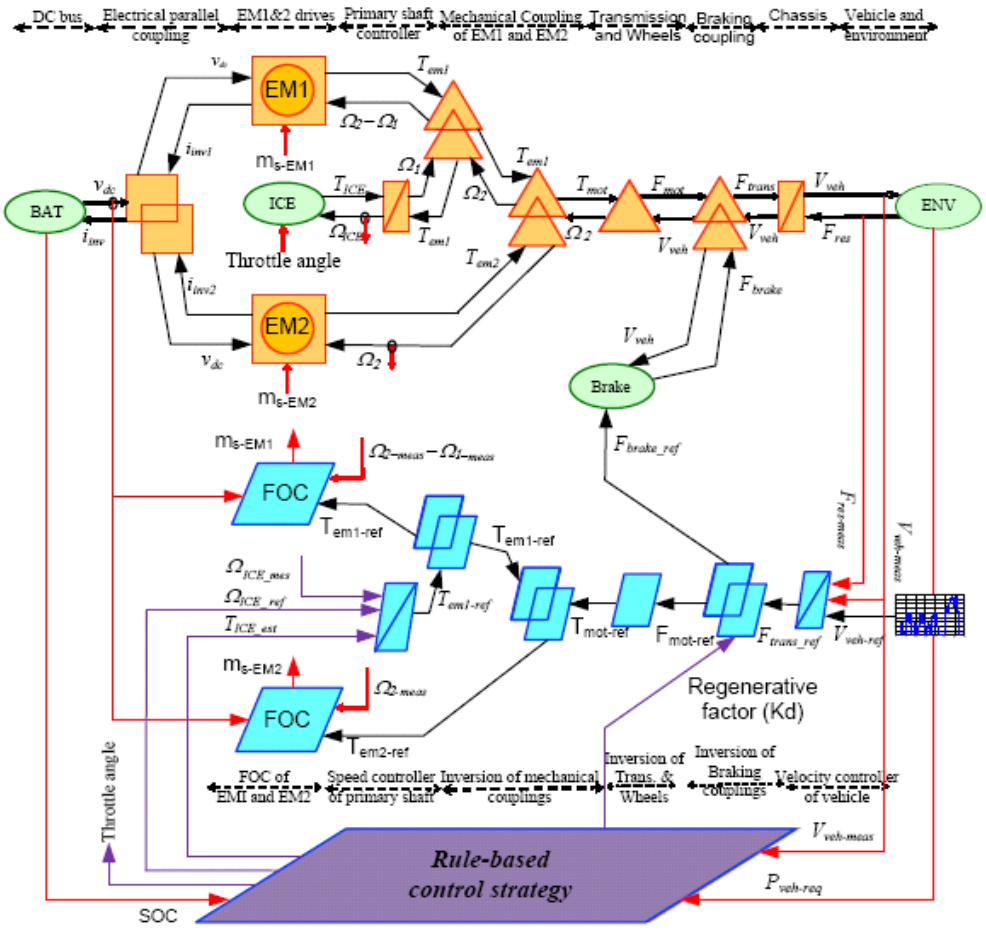


Fig. 4: EMR model of PMSM-EVT-HEV and the common control structure

$$V_{sdq\_ref} = C\left[i_{sdq\_ref} - i_{sdq\_meas}\right] + e_{sdq\_est} \qquad (19)$$

$$m_{EM} = \frac{u_{inv\_ref}}{V_{dc}} \qquad (23)$$

**Variables estimation:** In practice only stator currents and rotational speed are measured and the other variables are estimated such as $e_{sdq\_est}$:

$$e_{sd\_est} = -L_q i_{q\,meas}\left(\Omega_{s-meas} - \Omega_{r-meas}\right) \qquad (20)$$

$$e_{sq\_est} = \left(L_d i_{d\_meas} + \varphi_e\right)\left(\Omega_{s-meas} - \Omega_{r\_meas}\right) \qquad (21)$$

**Inversion of park transformation and index of the inverters:** it leads to reference voltages $u_{inv\_ref}$ from the (d-q) voltages; and the modulation index of the inverter is calculated using the measured battery voltage:

$$u_{inv\_ref} = \left[T(\Delta\theta)\right]^{-1} v_{sdq\_ref} \qquad (22)$$

**Integration of PMSM-EVT-HEV components:** Figure 4 shows the EMR simulation model for the studied HEV. It consists mainly into three sections. The first is the model of the vehicle components (battery, power inverters, power connectors, IC engine, transmission and PMSM-EVT machines). The second is the control system for each component, including the field weakening vector control for the EVT machines. More details could be found in (Cheng *et al*., 2008; Chen *et al*., 2008a; Letrouve *et al*., 2009; Cheng *et al*., 2009) for the HEV system with induction machines-EVT. Finally, the power follower rule-base control strategy is developed to revise the power distribution process between the ICE and the EVT machines.

## GLOBAL RULE-BASE CONTROL STRATEGY

The energy management strategy aims to fulfill predetermined requirements without knowledge of future

drive conditions. The first step to design the energy management strategy is to define the global strategy regarding the characteristics and constraints of the vehicle. In the developed rule-base power management strategy, the ICE at its power is considered the base driving plant and the developed power from EM2 is to cover the power difference between the ICE optimum power and the vehicle requirements. Hence, the control strategy comes to distribute the role study of each component on HEV system. The rule-based control strategy is briefly mentioned as follow:

**Power requested from the ICE:** The total power requested from the ICE is composed mainly to two parts. The first is the power required to drive the vehicle through EM1. The second is the power required to charge the battery via EM1. All power required from the engine is limited by its optimal operational region. The power lower than the minimum optimal limits; and also the power greater than the maximum optimum level will be excited by the EVT machines. These restrictions would be cancelled at the emergency cases.

The power drawn from the engine is mainly determined by two factors. The first is the predetermined target SOC such that the engine power varied between its optimum minimum and maximum power limits corresponding to the value of the SOC. The second is the requested power by the driver. If the vehicle power less than the optimum minimum level of ICE, the engine presents either no power or its optimum minimum power according to the SOC. But, if the vehicle power larger than the optimum minimum level of ICE, the engine will present at least its optimum minimum power reaching its maximum level according to the power requested.

**The ON/OFF control of the ICE:** The ON/OFF control of the ICE plays an important rule on the system. Although this control has to guarantee the operation on the optimum region, it has to prevent the frequently ON/OFF of the engine. Also, it sustains the SOC at its efficient target value.

**SOC of the battery:** SOC of the battery is controlled at predetermined target value to assure the dynamic answer and guarantee enough energy to accelerate the vehicle and enough capacity to recovery energy. Also, the designed control strategy has to minimize the DC bus voltage variation. Currents, powers and/or voltages (and change rates) must remain within predetermined limits. If the vehicle is at maximal speed, no further acceleration will be required and braking is the next state, a high SOC will limit the recovery of braking energy. Hence, the control strategy maintains the SOC on low level to increase the opportunity of energy recovery and exploiting the stored kinetic energy inside the running vehicle.

Table 4: Specifications of the used driving cycles

| CYC | Max. velocity km/h | Max acceleration m/s^2 | Max. deceleration m/s^2 |
|---|---|---|---|
| 1015-PRIUS | 70.75 | 1.19 | 1.45 |
| Modified-1015-PRIUS | 90.56 | 1.5 | 1.9 |

**Regenerative braking:** Regenerative braking is considered one of the most economic and efficient aspect in HEVs. One of the main global objectives of the energy management system is to recuperate the maximal amount of braking energy. In this study, 60% from total braking energy has been recovered to the battery via EVT machines (EM2).

**Inputs and outputs:** The energy management strategy only uses the following current-time information to compute the output power references: vehicle velocity, power requested at the wheels, SOC and battery voltage. The energy management system has the following two outputs: optimum operational ICE power and the regenerative braking factor. The energy management rule-based control strategy has been implemented using the EMR in Matlab/ Simulink as shown in the lower part of Fig. 4.

## DISCUSSION AND ANALYSIS OF THE SIMULATION RESULTS

For the studied HEV system, simulation is carried out with two driving cycles: CYC-1015-6PRIUS and the modified CYC-1015-6PRIUS as listed in Table 4.

The simulation results through one-trip two driving cycles are shown in the following figures. From the simulation results, the power ratings of the EVT machines are checked via the densest operating points. The performance and ratings of vehicle dynamics, ICE, battery, EM1 and EM2 have been analyzed and discussed in details in the following subsections.

**Vehicle performance:** The simulation results for the vehicle are presented and analyzed in Fig. 5. The simulation results show that the simulation speed can tracking the driving cycle profile, in a way which indicates that the drive ability is satisfied Fig. 5a. In Fig. 5b, the power requested at the wheels is also presented showing the driving and regenerative powers. It shows that, for the used driving cycle, the maximum power requested is 28.52 kW; whereas the maximum negative power is 23 kW. Also, the maximum total torque is 160 Nm at the modified Prius cycle as in Fig. 5c.

**ICE performance:** Figure 6 shows the simulation results of the engine torque, speed and power. It can be seen that the torque, speed and power of the ICE with the control strategy varies into the predefined optimum ranges. Also seen in Fig. 7, the ICE operating points indicating that the

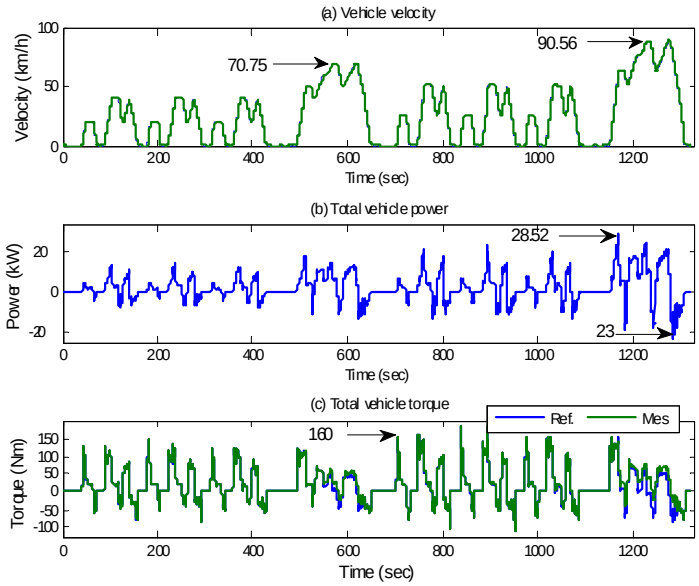


Fig. 5: Vehicle performance, (a) vehicle velocity, (b) vehicle power required at the wheels and (c) total torque

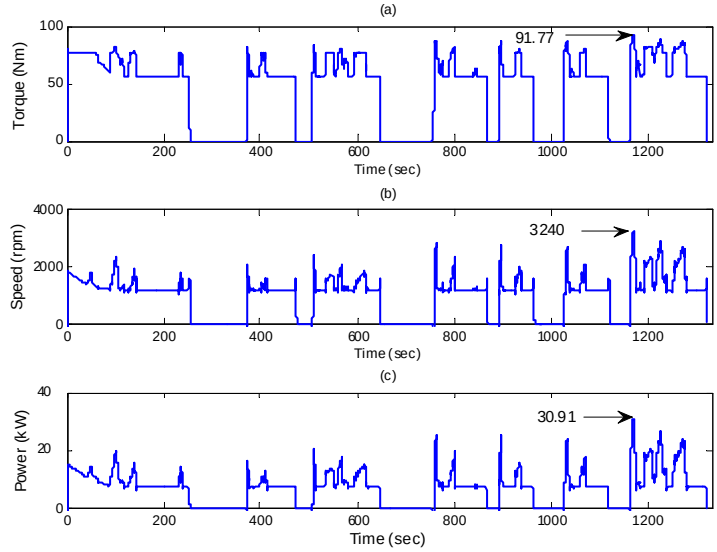


Fig. 6: Torque, speed and power flow on the ICE

engine, all of time, operates in its high- efficiency area. Also, the figures show the minimum and maximum optimum ratings of the engine: torque (55:91.77) Nm, speed (1200:3240) rpm, power (7:30.91) kW.

**EM2 performance:** Figure 8 shows the torque, speed, power flow and d-q currents of the outer PMSM (EM2). It is noted that the developed positive or negative torque can be determined according to the torque of ICE and vehicle requested torque. Seen in the same figure, the speed of EM2 proportionally aligned to the vehicle velocity. Also, it can be seen that the motor/generator, EM2. Most of the time, it studies in the generating mode because of the ICE and then EM1, all times, develops positive torque. Also, the figures show the minimum and maximum optimum ratings of EM2: maximum torque (160) Nm, speed (0:3290) rpm, power (-26.17:16) kW. Finally, when the speed becomes higher than the base speed, the direct component current takes a negative value to weak the field in the constant power region as shown in Fig. 8d.

**EM1 performance:** Figure 9 shows the torque, speed, power flow and d-q currents of the inner PMSM (EM1).

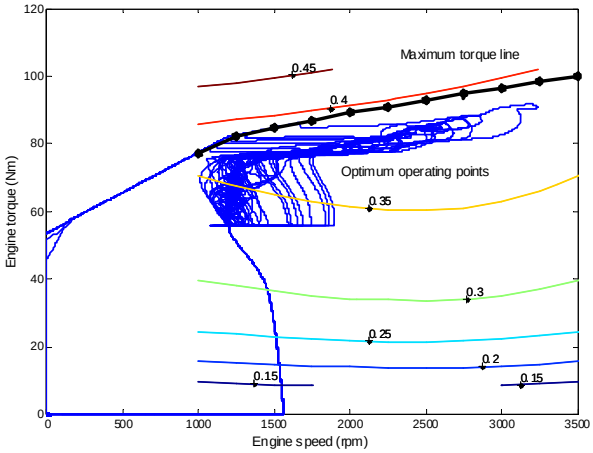


Fig. 7: Engine operation points

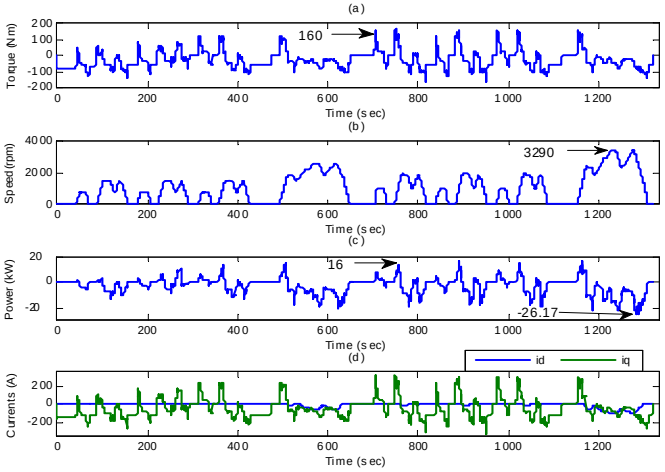


Fig. 8: Torque, speed, power flow and d-q currents of EM2

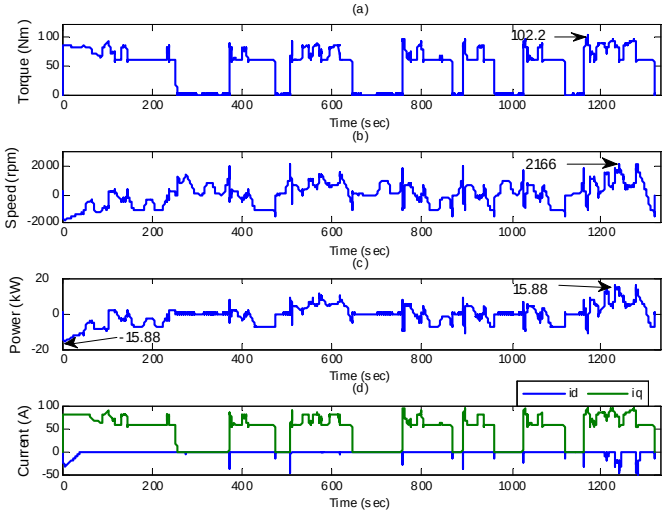


Fig. 9: Torque, speed, power and d-q currents of EM1

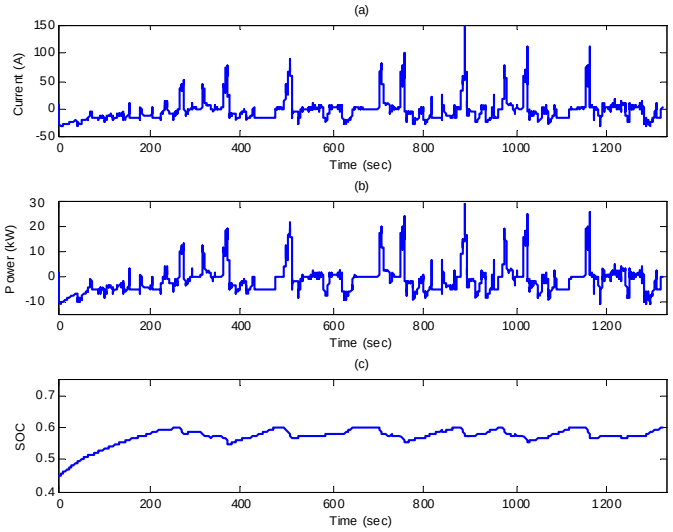


Fig. 10: Power and SOC of the battery

Table 5: Specifications of PM-EVT machines from the simulation results compared to PMSM-M/G

| | | THS-M/G | | PMSM-EVT | |
|---|---|---|---|---|---|
| Toyota prius | | MG1 | MG2 | EM1 | EM2 |
| Maximum power | kW | 15 | 30 | 15.88 | 26.17 |
| Maximum torque | Nm/rpm | 58@2470 | 305@940 | 105 @0-1378 | 160 @0-1720 |
| Maximum speed | rpm | - | - | 2578 | 4300 |

It is noted that the developed torque is positive and slightly larger than the ICE torque because of the dynamic inertia. Also, it can be seen that the speed of EM1 equals to the difference between the ICE and EM2 speeds. Positive or/and negative speed is related to the vehicle's velocity and ICE operation. Also, it can be seen that the peaking power in the figure (15.88) kW occurs at the maximum vehicle speed of 90.56 km/h. Also, when the speed becomes higher than the base speed, the direct component current takes a negative value to weak the field in the constant power region as shown in Fig. 9d.

**Battery performance:** The simulation results for the battery are presented and analyzed below. For this simulation, the initial SOC value is set to 0.45. The favorable range of SOC is 0.6. Shown in Fig. 10, the SOC is sustained at the desired value. In this figure, the value of battery power is also presented. Also, the graph of battery SOC adequately shows charging state by regenerative braking during deceleration.

## CONCLUSION

In Toyota prius HEV, THS transmission system has been replaced by the PMSM-EVT with achieving all worst dynamic conditions. Optimum operation of the engine, good performance of the battery and decreasing the power ratings of the electrical machines have been achieved via the presented control strategy. This has been done by two aspects: the first is optimum parametric design of the EVT machines which has been achieved by the union of the calculation method and the simulation results. The second is the robust control of the EVT machines including the field weakening operation. The power parameters of the PMSMs have been saved relating to the PMSM-M/G on the Toyota prius HEV as listed in Table 5.

## REFERENCES

ADVISOR, Advanced Vehicle Simulator, 2002. National Renewable Energy Laboratory (NREL) of U.S. Department of energy.

Chau, K.T., C.C. Chan and C. Liu, 2008. Overview of permanent-magnet brushless drives for electric and hybrid electric vehicles. IEEE Trans. Indus. Electr., 55(6): 2246-2257.

Chen, K., Y. Cheng, A. Bouscayrol, C.C. Chan, A. Berthon and S. Cui, 2008(a). Inversion-Based Control of a Hybrid Electric Vehicle Using a Split Electrical Variable Transmission. IEEE Vehicle Power and Propulsion conference, VPPC, pp: 1-6.

Chen, K., A. Bouscayrol and W. Lhomme, 2008(b). Energetic macroscopic representation and inversion-based control: Application to an electric vehicle with an electrical differential. J. Asian Electric Vehicles, 6(1).

Chen, K., W. Lhomme, A. Bouscayrol and A. Berthon, 2009. Comparison of Two Series-Parallel Hybrid Electric Vehicles Focusing on Control Structures and Operation Modes. IEEE Vehicle Power and Propulsion Conference, VPPC, 1308-1315.

Cheng, Y., K. Chen, C.C. Chan, A. Bouscayrol and S. Cui, 2008, Global Modelling and Control Strategy Simulation for a Hybrid Electric Vehicle Using Electrical Variable Transmission. Proceedings of IEEE VPPC, China.

Cheng, Y., S. Cui and C.C. Chan, 2009. A novel series-parallel power train for hybrid electric vehicle applications. J. Asian Electric Vehicles, 7(1), 1239-1244.

Cheng, Y., T. Rochdi, E. Christophe, A. Bouscayrol and S. Cui, 2011. Specifications and design of a pm electric variable transmission for toyota Prius II. IEEE T. Veh. Technol., 60(9): 4106-4114.

Ehsani, M., Y. Gao and A. Emadi, 2010. Modern Electric, Hybrid Electric and Fuel Cell Vehicles: Fundamental, Theory and Design. 2nd Edn., CRC Press, Taylor and Francis Group.

Fan, T., X. Wen, C. Jingwei and G. Xizheng, 2008. Permanent Magnet Dual Mechanical Port Machine Design for Hybrid Electric Vehicle Application. IEEE International Conference on Industrial Technology, ICIT, pp: 1-5.

Guo, X., X. Wen, F. Zhao and T. Fan, 2008. Power parameters matching design of dual mechanical ports electric matching design of dual mechanical ports electric machine with clutch applied in hybrid electric vehicle. Proceeding ICEMS, pp: 3595-3599.

Krishnan, R., 2010. Permanent Magnet Synchronous and Brushless DC Motor Drives, Taylor and Francis Group, LLC CRC Press, pp: 293-303.

Kruse, R., S. Mourad, D. Foster and M. Hoeijmakers, 2006. Concept and functionalities of the electric variable transmission. Aachener Koloquium Fahrzeug-und Motoretechnik, 15(Aachen): 1387-1398.

Letrouve, T., P. Delarue and A. Bouscayrol, 2009. Modelling and Control of a Double Parallel Hybrid Electric Vehicle Using Energetic Macroscopic Representation. ELECTROMOTION, EPE Chapter lectric Drives Joint Symposium, 1-3, Lille, France.

Liu, J., H. Peng and Z. Filipi, 2005. Modeling and analysis of Toyota hybrid system. Proceedings IEEE/ASME International Conference on Advanced Intelligent Mechatronics, pp: 134-139.

Zhuang, X., W. Xuhui, Z. Feng, F. Tao and G. Xinhua, 2009. An optimal method of power parameters matching design in DMPM based HEV. International Conference on Electrical Machines and Systems, pp: 1-6.